Acta Sci. Pol.
Architectura 23 (2024), 384–397
aspa.sggw.edu.pl ISSN 1644-0633 (suspended) eISSN 2544-1760 DOI: 10.22630/ASPA.2024.23.30

ORIGINAL PAPER

Received: 02.07.2024
Accepted: 20.10.2024

SEEPAGE ANALYSIS OF THE MAMAK DAM, INDONESIA: A CASE STUDY

Noor Halim✉, Zbigniew Lechowicz, Mirosław Lipiński

Institute of Civil Engineering, Warsaw University of Life Sciences – SGGW, Warsaw, Poland

ABSTRACT

In general, the current performance evaluation of the Mamak Dam falls into the "fairly good" category, even in the aftermath of the earthquake event with a magnitude of 6.5 Mw in 2018. However, the presence of leakage on the downstream slope has become an issue that requires attention. This study analyses seepage using GeoStudio and Slide Rocscience software. The seepage rates obtained from instrument readings exceed those calculated by GeoStudio and Slide Rocscience software. All of the obtained seepage rate results do not surpass the maximum allowable seepage rate requirements. The most critical gradients are from flood water level cases in Saddle Dam-1 and Saddle Dam-2. They reached values of 0.35 and 0.34, which fall below the maximum hydraulic gradient.

Keywords: seepage rate, instrument readings, hydraulic gradient

INTRODUCTION

Dams pose a high level of danger to both human lives and property in the event of structural damage or breaches in their structures (Sujono, 2012). Samekto and Azdan (2008) suggest that failures in dams can occur due to various factors (Utepov et al., 2022). Primary causes of dam failure include water overflow (overtopping), water leakage, landslides (dam stability) and other factors such as earthquakes, liquefaction or sabotage according to the International Commission on Large Dams (ICOLD, 2018, 2019). Among these causes, water seepage is the most frequent accounting for 43% of dam failures. When a dam structure fails, it is often due to water leaking, leading to serious problems and potential disasters.

One of the leading causes of embankment dam failure is water leakage, leading to a process known as "piping", which disrupts the dam's stability and safety. To prevent hazardous water leakage, monitoring and assessing dam leakage condition is essential. This is typically done using instruments like piezometers placed on the dam's body and drainage systems (v-notch) installed downstream as a toe drain (Foster, Fell & Spannagle, 2000).

The amount of water leakage is influenced by factors such as material permeability coefficient (k), hydraulic gradient (i) and water level in the reservoir (Δh), (Wulandari & Tjandra, 2019).

Water leakage increases as the pressure on the dam rises, and the time for water to seep through shortens (Nurnawaty, Suhardiman & Ihwan, 2018). Rising water levels in the reservoir elevate pressure inside the dam's pores, causing more water leakage (Huda, Wardani & Suharyanto, 2019). Variations in water levels

Noor Halim https://orcid.org/0009-0009-2854-5022; Zbigniew Lechowicz https://orcid.org/0000-0002-1426-5881;
Mirosław Lipiński https://orcid.org/0000-0002-6235-8185
✉halymnoor@gmail.com

impact the pressure within the dam's pores. Rainfall intensity influences the pore water pressure on the dam's upstream slope, with heavier rainfall resulting in more significant variations in pressure (Huda et al., 2019).

The Indonesian Dam Safety Commission's study on 122 embankment dams revealed that 20% are considered at risk. Among these vulnerable dams, 59% have been in operation for over 25 years, while the remaining 41% are younger than 25 years (Komisi Keamanan Bendungan [KKB], 2020).

The aim of the paper is to analyse the behaviour of the Mamak Earth Dam in Indonesia by assessing the filtration process in complex geological, geotechnical and seismic conditions. The basics of analysing the filtration process through earth dams are presented, considering the impacts, flow conditions and filtration safety criteria. The filtration process through the main dam, saddle dams and abutments was evaluated based on the results of numerical analysis using GeoStudio and Slide Rocscience software to determine seepage rates and hydraulic gradients. These results were then compared with the available measurements from the control system.

LITERATURE REVIEW

Theory of seepage

Due to changes in pressure and elevation, groundwater moves towards areas of lower potential energy. The total head, commonly used to quantify potential energy (UE), is essentially the combined value of pressure head and elevation head. The differential form of Darcy's law indicates that the flow rate per unit area is directly proportional to the rate at which the head changes. The subsequent fundamental equation governing seepage through earth dams can be regarded as (Elshemy, Nasr, Bahloul & Rashwan, 2002; Ismail, Ng & Gey, 2012):

$$\frac{\partial}{\partial x}\left[k_x \frac{\partial H}{\partial x}\right]+\frac{\partial}{\partial y}\left[k_y \frac{\partial H}{\partial y}\right]+\frac{\partial}{\partial z}\left[k_z \frac{\partial H}{\partial z}\right]=S\frac{\partial h}{\partial t}, \tag{1}$$

where:

kx, k_y, k_z – coefficients of permeability in x, y and z directions, respectively [-],
S – specific yield [-],
H – total fluid head ($H = p/\gamma_w + z$) [m],
p – pressure [Pa],
γ_w – unit weight of water [kN·m^{-3}],
z – elevation head [m].

Equation (1) is commonly referred to as Laplace's equation, serving as the fundamental equation for modelling three-dimensional groundwater flow in aquifers. When considering a steady-state scenario in an isotropic and homogeneous aquifer, Equation (2) can be simplified to the following expression:

$$\frac{\partial^2 H}{\partial x^2}+\frac{\partial^2 H}{\partial z^2}=0. \tag{2}$$

The assumptions made are as follows: the soil media is homogeneous, isotropic and physically stable; atmospheric pressure prevails throughout the water table (phreatic surface); the flow of groundwater through the flow domain is steady and the hydraulic conductivity within the embankment remains constant throughout.

This study uses Seep/W function of GeoStudio software to model water seepage from a reservoir through an earth dam while calculating the factor of safety (FoS) against slope failure using the simplified

Bishop's method and considering various soil conditions. The fundamental differential equation that governs two-dimensional seepage can be formulated as follows:

$$\frac{\partial}{\partial x}\left(k_x \frac{\partial H}{\partial x}\right)+\frac{\partial}{\partial y}\left(k_y \frac{\partial H}{\partial y}\right)+Q=\frac{\partial \theta}{\partial t}, \tag{3}$$

where:
Q – flow rate [$m^3 \cdot s^{-1}$],
θ – water content volume [m^3].

Equation (3) illustrates that the disparity between the inflow and outflow rates corresponds to the alteration in the storage of soil systems.

There are two fundamental categories of seepage analysis: steady-state seepage, which models the behaviour of reservoir water when it is at full storage; and transient-state seepage, which simulates the drawdown of reservoir water (Himanshu & Burman, 2019). The mathematical expressions associated with each type are as follows:

– for steady-state seepage:

$$\frac{\partial}{\partial x}\left(k_x \frac{\partial H}{\partial x}\right)+\frac{\partial}{\partial y}\left(k_y \frac{\partial H}{\partial y}\right)+Q=0, \tag{4}$$

– for transient-state seepage:

$$\frac{\partial}{\partial x}\left(k_x \frac{\partial H}{\partial x}\right)+\frac{\partial}{\partial y}\left(k_y \frac{\partial H}{\partial y}\right)+Q=m_w \gamma_w \frac{\partial (H)}{\partial t}, \tag{5}$$

where:
H – total available hydraulic head difference [m],
t – time factor [s],
Q – applied boundary flux (discharge) [$m^3 \cdot s^{-1}$],
m_w – slope of the storage curve [°].

Boundary conditions

Figure 1 is a diagrammatic illustration of the problem statement and boundary conditions for a typical earth dam.

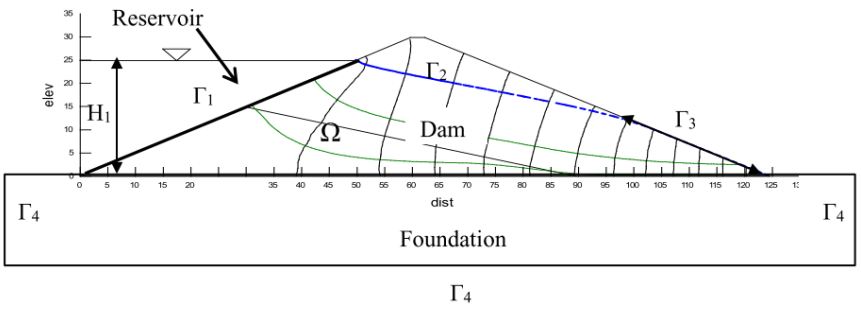

Fig. 1. Problem statement and boundary conditions

Source: Kirra et al. (2015).

These boundary conditions can be briefly summarised as follows:

– Entrance surface (Γ1): the upstream boundary surface, denoted as Γ1, serves as the entry point where water begins to permeate through the material. This surface is regarded as an equipotential line, referred to one of Dirichlet's condition, specifying a predetermined head:

$$H(x, y) = H_1. \tag{6}$$

– Phreatic surface (Γ2): the boundary surface labelled as Γ2, representing the path of flow through the dam, corresponds to the phreatic surface. This separation line is seen as a streamline. While the phreatic surface is regarded as a boundary condition, its exact location and shape are initially uncertain. In the case of the unknown phreatic surface, the boundary condition is as follows:

$$H(x, y) = y, \tag{7}$$

$$\frac{\partial H}{\partial n} = y, \tag{8}$$

where:
n – normal directions to the boundary (Γ2).

– Exit surface (seepage surface) (Γ3): the boundary surface, denoted as Γ3, functions as the exit surface or seepage surface. This boundary is treated as an isobar, where the pressure is atmospheric along its length. Consequently, the boundary condition associated with such a surface is:

$$H(x, y) = y. \tag{9}$$

The configuration of the seepage surface is understood, except for its upper boundary, which is the exit point situated on the unknown phreatic surface. Determining the location of this specific point is essential for finding a solution.

– Dam foundation boundary (Γ4): the boundary surface, referred to as Γ4, represents the dam's foundation boundary and is associated with the Neumann boundary condition. In this study, this boundary is assumed to be impermeable, meaning it obstructs the flow of water across it. Consequently, the condition is defined as follows:

$$\frac{\partial H}{\partial n} = y, \tag{10}$$

where:
n – normal direction to the boundary (Γ4).

Safety criteria

In the Seep/W function of GeoStudio software, the amount of water that seeps out from the dam body to the downstream area is calculated by multiplying the average seepage water volume with the width of the dam for each metre. According to Indonesian guidelines, the calculation focuses on the cross-section that has the deepest part of the dam using the following equation:

$$Q_h = q_h \cdot A \cdot B, \tag{11}$$

where:
Q_h – seepage flow rate [$m^3 \cdot s^{-1}$],
q_h – average water flow [$m^3 \cdot s^{-1}$],
A – zone area [m^2],
B – width of the base area of the foundation [m].

The safety criteria of seepage analysis in the dam body is defined as follows:

$$i_c = \frac{\gamma'}{\gamma_w} = \frac{G_S - 1}{1 + e}, \tag{12}$$

$$FoS = \frac{i_c}{i_e} > 4, \tag{13}$$

where:
i_c – critical discharge gradient [-],
γ' – effective unit weight (submerged) [$kN \cdot m^{-3}$],
G_s – specific gravity unit weight [-],
e – void ratio [-],
i_e – exit gradient from seepage analysis or instrument measurement data [-],
FoS – factor of safety [-].

The parabolic equation of seepage line is defined by the following equation:

$$y_0 = \sqrt{\left(h^2 + d^2\right)} - d. \tag{14}$$

The design aims to manage leakage to an acceptable level. Quies (2002) defined guidance on typical seepage losses from earth dams, which is provided in Table 1.

Table 1. Guidance on typical seepage losses from earth dams

Dam height [m]	Seepage [L/min/m]	
	permissible	impermissible
< 5	< 25 (0.02)	> 50 (0.03)
5–10	< 50 (0.03)	> 100 (0.07)
10–20	< 100 (0.07)	> 200 (0.14)
20–40	< 200 (0.14)	> 400 (0.28)
40 >	< 400 (0.28)	> 800 (0.56)

Source: Quies (2002).

Meanwhile, regarding the hydraulic gradient, according to DIN 19700-12 (Deutsche Institut für Normung [DIN], 2004), as cited in Ersoy and Haselsteiner (2018), the critical gradient (i_c) for the present sand-gravels should be approximately to 0.20–0.40. For fine sands, this can decrease to 0.15, and for silts, it can be as low as 0.10 or even less.

CHARACTERISTICS OF THE MAMAK DAM

The Mamak Dam, constructed in 1990 on Sumbawa Island, Indonesia, has undergone continuous inspections throughout its 30-year operational period to address potential issues and mitigate the risks associated with water seepage, a critical concern for dam safety. This study examines seepage in the Mamak Dam, with a focus on its safety. Monitoring data from instruments such as piezometers and drainage systems (v-notches) are employed to observe water behaviour and compare the analysis results. According to the PT. Raya Konsult (2022b), the first v-notch system accumulates seepage from the main dam, while the second v-notch system accumulates seepage from Saddle Dam-1, measuring the amount of seepage flow on the measured seepage rate is based.

The Mamak Dam serves multiple functions, including hydropower generation, irrigation and local water supply. It has four embankments: the main dam, Saddle Dam-1, Saddle Dam-2 and Saddle Dam-3 (Fig. 2). The structure of Mamak Dam consists of several essential elements, including the impervious core (constructed from earth fill), a filter layer, a transition layer, random rock, selected rock and rock fill. The specifications of the Mamak Dam are provided in Table 2.

Fig. 2. Bird's view of the Mamak Dam

Source: PT. Raya Konsult (2022a).

Table 2. Salient features of the Mamak Dam

Description	Unit measurement	Value
Reservoir		
Catchment area	km^2	108
Gross storage at FWL	million m^3	29.839
Live storage capacity	million m^3	27.671
Dead storage capacity	million m^3	2.167
Water spread area at FWL	km^2	2.357
Flood water level (FWL)	m	elevation +95.40

Table 2 (cont.)

Description	Unit measurement	Value
Normal water level (NWL)	m	elevation +93.43
Low water level (LWL)	m	elevation +74.00
Deepest bed level	m	elevation +58.00
Design flood discharge (probable maximum flood)	$m^3 \cdot s^{-1}$	664 (0.5 PMF)
Main dam + cofferdams		
Height	m	36.959
Crest level	m	elevation +99.93
Length	m	203.01
Crest width	m	10.66
Saddle Dam-1		
Height	m	33.929
Crest level	m	elevation +99.93
Length	m	205.394
Crest width	m	10.245
Saddle Dam-2		
Height	m	10.929
Crest level	m	elevation +99.56
Length	m	54.611
Crest width	m	9.832
Saddle Dam-3		
Height	m	16.538
Crest level	m	elevation +99.80
Length	m	85.986
Crest width	m	10.154

Source: PT. Raya Konsult (2022b).

Seepage in Saddle Dam-1 and Saddle Dam-2

Based on geoelectric investigation, the seepage in Saddle Dam-1 is likely to originate from pockets of water present on the surface of Saddle Dam-1 because there is an indication of low resistivity at the surface. Low resistivity on the surface of the downstream slope indicates rock softening, which affects the permeability of the soil near the seepage point (Fig. 3a). Seepage in Saddle Dam-2 is observed to flow from the deformation zone (Zone C) through the pores of softened rock (northern part of Zone I), then exit through Zone E (seepage). This means there is a water connection pathway from the curved area on the crest to the seepage point on the downstream side. The deflection contributes to the seepage only when Zone C is filled with water (Fig. 3b).

a

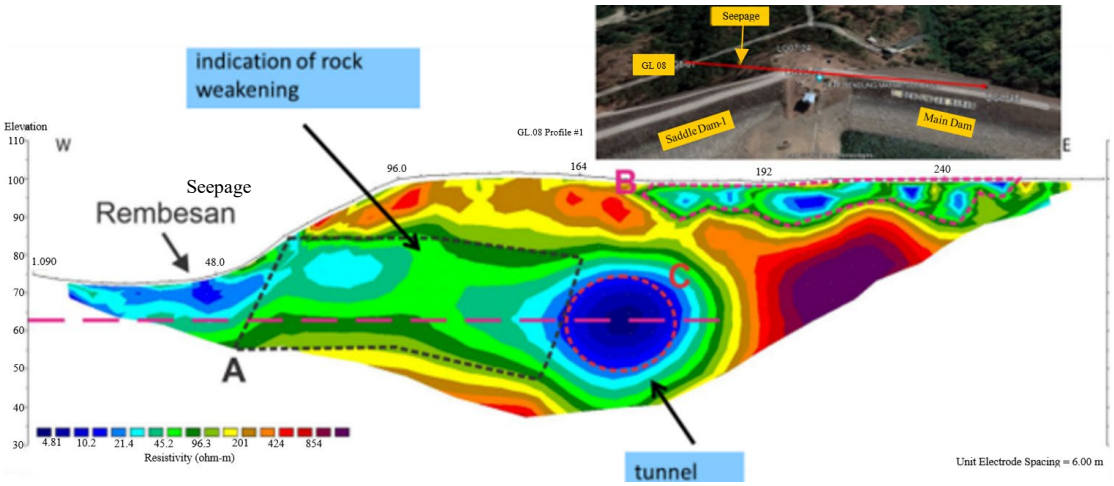

b

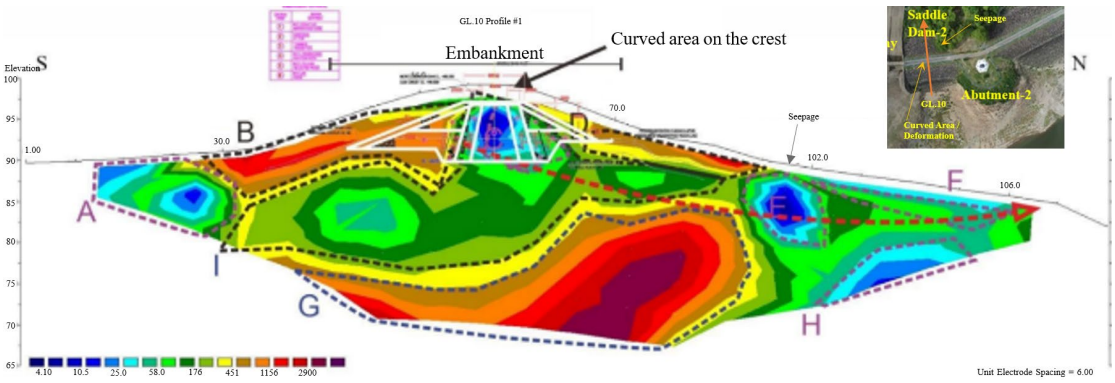

Fig. 3. Geoelectric investigation: a – Geoelectric survey Line 8 (GL8) in Saddle Dam-1, b – geoelectric survey Line 10 (GL10) in Saddle Dam-2

Source: PT. Raya Konsult (2022a).

Geotechnical design parameters

In the process of constructing a numerical model, the next stage involves allocating materials to the regions within it. The key factors for seepage analysis are the geotechnical parameters.

The geotechnical parameters of the main dam, Saddle Dam-1, Saddle Dam-2, Abutment-1 and Abutment-2, which are incorporated in the numerical model, are presented in Table 3. The cross-sections for the analysis are illustrated in Figure 4.

Table 3. Geotechnical parameters of the Mamak Dam

Type	Zone	Soil classification	Saturated permeability coefficient (k_s) [m·s^{-1}]	Zone area ($A = k_y/k_x$) [-]	Unit weight (γ) [kN·m^{-3}]	Effective cohesion (c') [kPa]	Effective angle of friction (φ') [°]
Embankment zone	earth-fill zone	clay	5.82E-06	0.5	17.52	12.00	27.10
	filler zone	sand	3.28E-03	1.0	20.90	0	32.00
	transition zone	sand	3.60E-02	1.0	18.09	0	28.14
	random zone	clay	3.80E-04	1.0	18.90	6.00	30.10
	selected rock	rock	–	1.0	18.67	0	37.00
	rock-fill zones	rock	–	0.4	21.70	4.15	36.15
	rip-rap	rock	3.30E-03	1.0	25.00	5.00	37.00
Abutment	Abutment-1 Abutment-2	clay	1.00E-04	1.0	17.11	2.30	28.75
Foundation	downstream area	clay	1.00E-04	1.0	18.00	35.00	41.00
	below DS	sandy clay	1.00E-04	1.0	17.04	10.00	32.00

Source: PT. Raya Konsult (2022a).

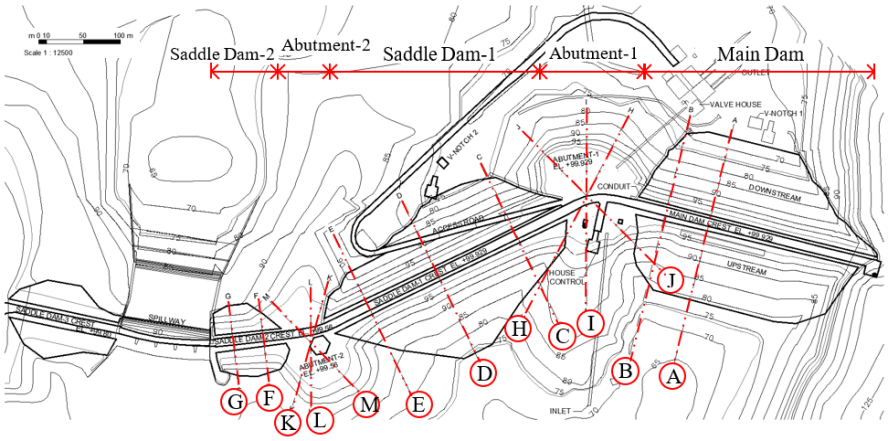

Fig. 4. Location of the cross-sections on the dam plane for seepage analysis

Source: Halim (2023).

To ensure accurate inputs for the numerical model, the geotechnical parameters are incorporated in accordance with construction material data and laboratory test results from soil samples taken in the ground field. To provide a refined set of inputs for the numerical model, the geotechnical parameters are organised based on the designated zones typically found in embankment dams.

Verification model

The assessment of stability is conducted for both the slopes on the upstream and downstream sides of the Mamak Dam embankment. Then, the outcomes of the analysis are compared with the safety standards and guidelines. The view of one of the numerical models (Cross-section A) is given in Figure 5.

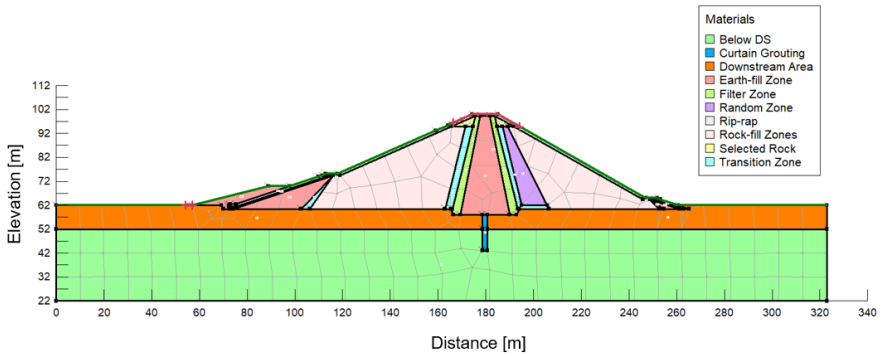

Fig. 5. Finite element model for seepage analysis (Cross-section A)

Source: GEO-SLOPE International (2023).

To investigate seepage flow under stable (steady state) conditions within the embankment, the finite element method (FEM) necessitates the specification of boundary conditions. Three hydraulic boundary conditions are applied for the numerical model as follows:

1. Constant head in the upstream face at a height of 71.2 m (NWL) with 31.2 m above the terrain surface. It can be seen in the pink line in Figure 5.
2. Constant head in the downstream face at the normal water level, which is at a height of 40 m. It can be seen in the yellow downstream line in Figure 5.
3. Seepage exit, which has a total flux type for a boundary. Potential seepage areas exit along the downstream slope have the groundwater flow as 0 $m^3 \cdot s^{-1}$. It can be seen in the red line in Figure 5.

ANALYSIS OF RESULTS

Seepage analysis results

In each case, the results from instrument readings report significantly higher seepage rates compared to the results of GeoStudio and Slide Rocscience software. This is due to certain conditions of the materials within the embankment of Saddle Dam-1 and Saddle Dam-2. In Saddle Dam-1, low resistivity on the surface of the downstream slope indicated rock softening, which affects the permeability of the soil near the seepage point. Conversely, Saddle Dam-2 has a water connection pathway from the curved area on the crest to the seepage point on the downstream side, thus causing the seepage rate from instrument readings to be higher than the results of GeoStudio and Slide Rocscience software (Table 4).

Table 4. Seepage rate in the downstream side

Dam part	GeoStudio software			Slide Rocscience software			PT. Raya Konsult (2022)	
	NWL (93.43 m) [$m^3 \cdot s^{-1}$]	FWL (95.40 m) [$m^3 \cdot s^{-1}$]	LWL (74.00 m) [$m^3 \cdot s^{-1}$]	NWL (93.43 m) [$m^3 \cdot s^{-1}$]	FWL (95.40 m) [$m^3 \cdot s^{-1}$]	LWL (74.00 m) [$m^3 \cdot s^{-1}$]	elevation 94.25 m [$m^3 \cdot s^{-1}$]	elevation 93.58 m [$m^3 \cdot s^{-1}$]
Main dam	7.03E-06	7.92E-06	3.31E-07	2.55E-07	2.57E-07	2.08E-07	3.28E-04[a]	–
Saddle Dam-1	1.44E-06	1.61E-06	1.13E-07	5.79E-07	6.02E-07	4.63E-07	2.62E-04[a]	1.90E-05[b]
Saddle Dam-2	8.85E-08	2.63E-07	–	4.63E-07	5.79E-07	–	–	2.60E-05[b]
Abutment-1	3.13E-05	3.03E-05	2.32E-05	5.56E-07	5.80E-07	4.40E-07	–	–
Abutment-2	7.01E-04	8.48E-04	–	6.02E-07	1.74E-07	–	–	–

NWL – normal water level, FWL – full water level, LWL – low water level.

[a]Seepage rate measured from v-notch.
[b]Seepage discharge was collected into a measuring cylinder through a pipeline from where the rate of seepage was calculated.

Source: Halim (2023).

However, each seepage rate has satisfied the requirement. In conclusion, the seepage that occurred in the Mamak Dam is considered to be safe. However, the presence of water seepage on the upstream slope creates a problem that requires local protection using a composite geosynthetic barrier and continuous observations.

Hydraulic gradient

The hydraulic gradients within the dam body are generally safe, $0.20 < i_c < 0.40$. The most critical gradients are from flood water level cases in Saddle Dam-1 and Saddle Dam-2, 0.35 and 0.34, respectively (Table 5). Thus, erosion through the dam body should not be a problem, except for Saddle Dam-2, where there is a water connection pathway from the curved area on the crest to the seepage point on the downstream side.

Table 5. Hydraulic and critical gradients

Dam part	Exit gradient (i_e) from GeoStudio [$m^3 \cdot s^{-1}$]			Exit gradient (i_e) from Slide Rocscience [$m^3 \cdot s^{-1}$]		
	NWL	FWL	LWL	NWL	FWL	LWL
Main dam	0.28	0.30	0.28	0.31	0.32	0.28
Saddle Dam-1	0.30	0.33	0.11	0.34	0.35	0.21
Saddle Dam-2	0.13	0.20	–	0.25	0.34	–
Abutment-1	0.27	0.33	0.13	0.17	0.30	0.15
Abutment-2	0.29	0.35	–	0.26	0.35	–

NWL – normal water level, FWL – full water level, LWL – low water level.

Source: Halim (2023).

This condition could potentially lead to the failure of the embankment in Saddle Dam-2. Therefore, it is necessary to address and reduce the risk of unforeseen hazards by installing a water-resistant barrier (a geocomposite consisting of a layer of natural sodium bentonite clay sandwiched between two geotextile layers (non-woven geotextile) or geomembrane (HDPE geomembrane) – Figure 6.

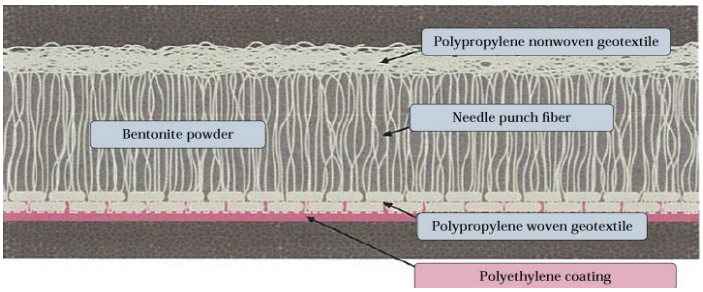

Fig. 6. Structural composition of geocomposite

Source: Koerner (2012).

The bentonite clay in GCLs has excellent swelling and self-sealing properties. When hydrated, the clay swells to create a watertight barrier and can self-heal if punctured. This makes GCLs an effective choice for reducing or eliminating local seepage in these applications.

CONCLUSIONS

The following conclusions have been drawn from the presented work:

– The seepage rates obtained from instrument readings exceed those calculated by the GeoStudio and Slide Rocscience analyses. This is due to certain condition of the materials within the embankment of Saddle Dam-1 and Saddle Dam-2. In Saddle Dam-1, low resistivity on the surface of the downstream slope indicated rock softening, which affects the permeability of the soil near the seepage point. On the other hand, Saddle Dam-2 has a water connection pathway from the curved area on the crest to the seepage point on the downstream side. These conditions should be modelled in the GeoStudio and Slide Rocscience numerical simulation to obtain more localised and accurate results. Nevertheless, each seepage rate result has satisfied the requirement. Therefore, the seepage problem in Saddle Dam-1 and Saddle Dam-2 is considered to be safe.
– The most critical gradients (i_c) come from flood water level cases in Saddle Dam-1 and Saddle Dam-2, where they are 0.35 and 0.34, respectively. However, the hydraulic gradients within the dam body were generally found to be safe as the required hydraulic gradient is $0.20 < i_c < 0.40$. Thus, erosion through the dam body should not be a problem, except for Saddle Dam-2 because of certain conditions within the dam body. This condition could potentially lead to the failure of the embankment in Saddle Dam-2. Therefore, it is necessary to address and reduce the risk of unforeseen hazards.
– To prevent the higher value of hydraulic gradients from being strong enough to continue the erosion process through the embankment and cause failure, it is suggested to install a water-resistant barrier/ /geocomposite consisting of non-woven geotextile, HDPE geomembrane and geosynthetic clay liner. The water-resistant barrier or geocomposite is positioned on the upstream slopes of both Saddle Dam-1 and Saddle Dam-2, as well as on the upstream slope of Abutment-1 and Abutment-2.

Acknowledgements

The research in the manuscript was supported by PT. Raya Konsult and PT. Virama Karya (Persero), Jakarta. We would like to extend our thanks to the authors from PT. Raya Konsult and PT. Virama Karya (Persero), Jakarta, for providing the necessary technical support.

Authors' contributions

Conceptualisation and methodology: Z.L., M.L. and N.H.; validation: N.H.; formal analysis: N.H.; investigation: N.H.; resources: N.H.; data curation: N.H.; writing – original draft preparation: N.H.; writing – review and editing: Z.L., M.L. and N.H.; visualisation: N.H.; project administration: N.H.

All authors have read and agreed to the published version of the manuscript.

REFERENCES

Deutsche Institut für Normung [DIN], (2004). *Stauanlagen. Teil 12: Hochwasserrückhaltebecken* (DIN 19700-12). Berlin: Deutsche Institut für Normung.

Elshemy, M., Nasr, R. I., Bahloul, M. M. & Rashwan, I. M. (2002). The effect of blockages through earth dams on the seepage characteristics. Faculty of Engineering, Tanta University, Egypt (Vol. 55, Issue June).

Ersoy, B. & Haselsteiner, R. (2018). *The seepage analysis of the embankment dams of a flood retention basin in Poland*. Marseille: Commission Internationale des Grands Barrages.

Foster, M., Fell, R. & Spannagle, M. (2000). The statistics of embankment dam failures and accidents. *Canadian Geotechnical Journal*, *37* (5), 1000–1024. https://doi.org/10.1139/t00-030

GEO-SLOPE International (2023). *Roads, Bridges and Embankments*. Calgary, Alberta, Canada. T2p 2Y5, Canada. Retrieved from: https://www.geoslope.com/solutions/roads-bridges-and-embankments [accessed: 01.07.2024].

Halim, N. (2023). A*nalysis of Mamak Dam behavior under different water levels in the reservoir* (MSc thesis). Warsaw University of Life Sciences, Warsaw.

Himanshu, N. & Burman, A. (2019). Seepage and Stability Analysis of Durgawati Earthen Dam: A Case Study. *Indian Geotechnical Journal*, *49* (1), 70–89. https://doi.org/10.1007/s40098-017-0283-1

Huda, A. L., Wardani, S. P. R. & Suharyanto, S. (2019). Evaluation of pore water pressure and water leakage in Panohan dam. *Reka Buana: Scientific Journal of Civil Engineering and Chemical Engineering*, *4* (2), 26. https://doi.org/10.33366/rekabuana.v4i2.1372

International Commission on Large Dams [ICOLD], (2018). *Flood Evaluation and Dam Safety*. Bulletin 170. Paris.

International Commission on Large Dams [ICOLD], (2019). *World Declaration on Dam Safety*. Porto.

Ismail, M. A. M., Ng, S. M. & Gey, E. K. (2012). Stability analysis of kelau earth-fill dam design under main critical conditions. *Electronic Journal of Geotechnical Engineering*, *17W*, 3209–3219.

Kirra, M. S., Zeidan, B. A., Shahien, M. & Elshemy, M. (2015). Seepage analysis of Walter F. George Dam, USA: A case study. *International Conference on Advances in Structural and Geotechnical Engineering. ICASGE'15*, *6*, 13. Retrieved from: https://www.researchgate.net/publication/280308070 [accessed: 01.07.2024].

Koerner, R. M. (2012). *Designing with Geosynthetics* (p. 118). Xlibris, USA. Retrieved from: https://www.scribd.com/read/523929953/Designing-with-Geosynthetics-6Th-Edition-Vol-1 [accessed: 01.07.2024].

Komisi Keamanan Bendungan [KKB], (2020). *Dam Operational Improvement and Safety Project (DOISP)*. The Indonesian Dam Safety Commission. Jakarta.

Nurnawaty, Suhardiman & Ihwan (2018). Analysis of water leakage in embankment dams (laboratory simulation test). *Jurnal Teknik Hidro*, *11* (1), 12–22. https://doi.org/10.26618/th.v11i1.2436

PT. Raya Konsult. (2022a). *Geological & geotechnical investigation report of Mamak Dam. In Preparation & Legalization of Dam Operational Permit in Sumbawa I Island*. Jakarta: Ministry of Public Works & Housing (MPWH).

PT. Raya Konsult. (2022b). *Hydrology report of Mamak Dam. In Preparation & Legalization of Dam Operational Permit in Sumbawa I Island*. Jakarta: Ministry of Public Works & Housing (MPWH).

Quies, L. (2002). *Guidance on typical seepage losses from earth dams*. Seepage Analysis. Retrieved from: http://what-when-how.com/Tutorial/topic-topic-8958bvhr/Geotechnical-Investigation-and-Design-Tables-225.html [accessed: 01.07.2024].

Samekto, C. & Azdan, M. D. (2008). *The critical condition of dams in Indonesia*. National Conference on Large Dams. Retrieved from: https://www.researchgate.net/publication/293491589 [accessed: 01.07.2024].

Sujono, J. (2012). Hydrological analysis of the Situ Gintung dam failure. *Journal of Disaster Research*, *7* (5), 590–594. https://doi.org/10.20965/jdr.2012.p0590

Utepov, Y., Lechowicz, Z., Zhussupbekov, A., Skutnik, Z., Aldungarova, A. & Mkilima, T. (2022). The Influence of Material Characteristics on Dam Stability Under Rapid Drawdown Conditions. *Archives of Civil Engineering*, *68* (1), 539–553. https://doi.org/10.24425/ace.2022.140184

Wulandari, P. S. & Tjandra, D. (2019). Analysis of the impact of reservoir water level fluctuations on dam slope stability using the PLAXIS 2D software. *Civil Engineering Communication Media*, *24* (2), 113. https://doi.org/10.14710/mkts.v24i2.17780

ANALIZA FILTRACJI PRZEZ ZAPORĘ MAMAK, INDONEZJA: STUDIUM PRZYPADKU

STRESZCZENIE

Ogólna ocena bieżącego stanu technicznego zapory Mamak wpisuje się w kategorię „akceptowalny" nawet po trzęsieniu ziemi o magnitudzie 6,5 Mw w 2018 roku. W artykule przeanalizowano reakcje zapory ziemnej Mamak w Indonezji pod kątem oceny przebiegu procesu filtracji w złożonych warunkach geologicznych, geotechnicznych i sejsmicznych. Przedstawiono podstawy analizy procesu filtracji przez zapory ziemne z uwzględnieniem występujących oddziaływań, warunków przepływu i kryteriów bezpieczeństwa filtracyjnego. Analizę procesu filtracji przeprowadzono z wykorzystaniem programów GeoStudio i Slide Rocscience. Prędkości przepływu uzyskane z odczytów instrumentów przekraczają obliczone z programów GeoStudio i Slide Rocscience. Wszystkie uzyskane wartości prędkości przepływu nie przekraczają maksymalnych dopuszczalnych prędkości przepływu. Najbardziej krytyczne gradienty występowały w przypadku podwyższenia poziomu wody podczas budowy grodzi 1 i grodzi 2. Osiągnęły one wartości 0,35 i 0,34, co jest poniżej maksymalnego gradientu hydraulicznego. Obecność przecieków wody na zboczu od strony odpowietrznej stwarza jednak problem, który wymaga lokalnego zabezpieczenia z wykorzystaniem kompozytowej bariery geosyntetycznej oraz ciągłych obserwacji.

Słowa kluczowe: prędkość przepływu, pomiary instrumentów, gradient hydrauliczny